TIME OF FLIGHT DIFFRACTION (TOFD) TECHNIQUE FOR ACCURATE SIZING OF EMBEDDED SUB CLADDING CRACKS

Sony Baby[1], T. Balasubramanian[1], R. J. Pardikar[2], M.Palaniappan[3] and R. Subbaratnam[3]
[1] Department of Physics, National Institute of Technology, Tamil Nadu, India, [2]NDTL, Bharat Heavy Electricals Limited, Tiruchirappalli, Tamil Nadu, India, and [3]Indira Gandhi Centre for Atomic Research, Kalpakam, Tamil Nadu, India

Abstract: This paper deals with an experimental study for evaluation of TOFD technique for determination of size of the embedded subcladding cracks. It extends the results presented in the previous papers [1, 2]. The study was confined to simulated cracks (machined slits) underneath the cladding. Crack heights ranging from 1.68mm to 19.04mm underneath Stainless Steel, Inconel and Ferritic cladding could be sized with an accuracy of ±0.2mm. Difficulty was experienced using TOFD to size cracks starting from the interface between Inconel /Stainless Steel cladding and the ferritic base i.e. (5mm/6mm below the scanning surface). However, these cracks could be well detected and sized by scanning through the cladding from the opposite surface of the blocks. Even the small cracks of the order of 1.9mm could be detected as long as they are not influenced by the lateral wave. Experimental errors are presented.

Introduction: In case of the welded structures, embedded vertical cracks are very often encountered necessitating reliable procedure for determining their size. Specialized ultrasonic techniques are required for estimation of through thickness height of these cracks [3-5]. The conventional pulse-echo technique have serious limitations for quantitative estimation of vertical cracks because it is subject to variations due to reflectivity, orientation of the defects, high attenuation of ultrasonic beam, cladding thickness etc., Therefore the study has been carried out to improve the accuracy of embedded crack height measurement based on transit time rather than the reflected amplitude using the Time-of-flight diffraction technique [6, 7].

In isotropic materials each type of elastic wave travels at its characteristic speed independent of direction. This is not so in anisotropic materials, where for any type of wave, the velocity depends on the direction with respect to the crystal axes of the material. Clearly for a technique such as TOFD, which relies on measurements of transit times, this adds an extra complication, which must be allowed for, if the technique is to maintain its accuracy. Studies of the propagation of ultrasound of austenitic weldments have been carried out by Silk [8-11].

Mathematical model for subcladding crack sizing: To calculate the defect depth (d) from the inspection surface, Pythagoras theorem is used [12]. Under the following assumptions
a). Crack is oriented in a plane perpendicular to both the inspection surface and the line joining the transmitter and receiver along the inspection surface.
b). Crack is midway between the transmitter and receiver.
The various ray paths are shown in Figure 1 and are associated with travel times given by:

$$t_a = \frac{2S}{V_g(90°)}$$

$$t_b = \frac{2S\sqrt{1+(h/S)^2}}{V_g(\phi)}$$

where the phase velocity direction ϕ is such that the group velocity θ satisfies the equation:

$$\theta = \tan^{-1}(S/h)$$

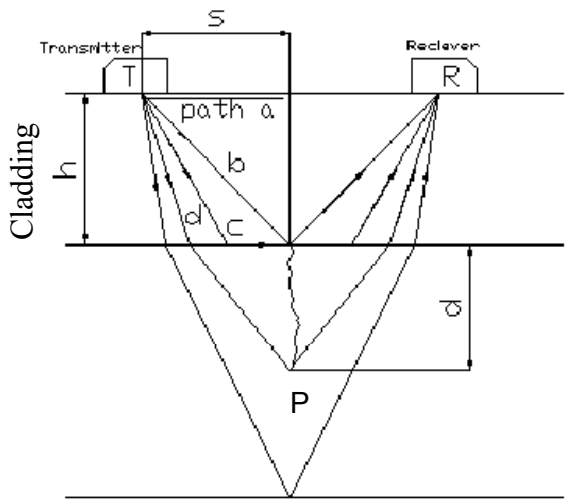

Figure 1: Ray paths into ferritic steel underneath austenitic / inconel cladding

Also

$$t_c = \frac{2h}{V_g(\varphi_0)\cos\theta_o} + \frac{2(S - h\tan\theta_0)}{V_f}$$

where θ_0 is the critical group velocity angle for the interface corresponding to the critical phase velocity angle ϕ_0 defined by

$$\sin\phi o = \frac{V_p(\phi_o)}{V_f}$$

The transit time via a point P, at a depth d below the interface, is given by t_d with

$$t_d = \frac{2h}{V_g(\varphi)\cos\theta} + \frac{2(S - h\tan\theta)\,V_p(\phi)}{V_f^2\sin\theta} \quad \text{---------} \quad (1)$$

where θ and ϕ are related to the defect depth by

$$d = (S - h\tan\theta)\,\frac{\sqrt{V_p^2(\phi) - V_f^2\sin^2\phi}}{V_f\sin\phi} \quad \text{----------} \quad (2)$$

For a point P' which is at distances S_t and S_r from transmitter and receiver respectively, the transit time from transmitter through P' to receiver is given by

$$t = \frac{[t_d(S_t) + t_d(S_r)]}{2}$$

where t_d is given by equation (1). Equations (1) and (2) define the relationship between depth and transit time in parametric form with the entry phase vector angle ϕ of the parameter.

Where d is the through wall extent of the crack, h is the thickness of the cladding, 2S is the distance of separation of the two probes, V_f is the velocity of the longitudinal wave in ferritic steel (independent of direction), $V_p(\theta)$ is the phase velocity of the longitudinal wave in austenite/inconel steel and $V_g(\theta)$ is the associated group velocity of the longitudinal wave in austenite/inconel steel.

The angle φ is, in both cases, measured relative to the normal to the inspection surface and is the angle that 'k' makes with the normal. The actual direction of the group velocity is, in general, at some other angle θ to the surface normal. The choice of reference path depends on the experimental conditions. For inspection of the region near to the clad surface, it is convenient to choose one of the paths a, b or c. A pulse traveling by path 'a' always arrives before one traveling via path 'b'. Path 'c' only exists for $S \geq h\tan\theta_0$. There is a value of S such that $t_a = t_c$ given by

$$S = \frac{H\,[V_g^{-1}(\phi_0)\cos\theta_0 - V_f^{-1}\tan\theta_0]}{V_g^{-1}(90°) - V_f^{-1}}$$

In practice, it is also usable down to $S = h\tan\theta \approx 3h$ because the amplitude received via path c is greater than that via path a.

Experiments using TOFD technique: Experimental study was carried out to determine what TOFD technique could achieve so far as the sizing of vertical/inclined subcladded cracks (machined slits) are concerned. TOFD equipment Model MICROPLUS of M/s AEA Technology, UK with manual scanner along with longitudinal angle beam probes of 45° - 4MHz was used for the study. The study was confined to simulated cracks. The steel test blocks used for the study contained 0.5mm wide vertical / inclined cracks (10°, 15°) inclination of various heights ranging from 1.68mm to 19.04mm underneath the Stainless steel, Inconel and Ferritic cladding. The slits were all smooth and varied in through wall extent. The actual dimensions of the block, the location and size of the simulated cracks (slits) is shown in Figure 2. Figure 3 shows the actual block after embedment of the simulated cracks (slits) by cladding. Slits are claimed to be really quite good models of cracks from the diffraction point of view [(13)].

Cladding of test blocks for embedment of simulated cracks (slits): Following procedures were used for embedding the cracks:

Stainless Steel cladding on carbon steel blocks: The first layer of the cladding was done very carefully using SMAW process, with E 309, φ 4mm electrode, Current: 130-140Amps, Voltage: 22-24V and preheating to 150°C. However for subsequent layers the electrode used was E 347 without preheat. The interpass temperature was maintained at maximum 120°C.

Ferritic cladding on carbon steel blocks: The cladding was done using SMAW process, with E 7018, φ 4mm electrode, by preheating to 150°C. The tempering bead was necessary to reduce HAZ.

Inconel cladding on carbon steel blocks: The first layer of the cladding was done very carefully using SMAW process, with UTP 068 HH, φ 4mm electrode, Current: 130-140Amps, Voltage: 22-24V and preheating to 150°C. However for subsequent layers no preheating was required. The interpass temperature was maintained at maximum 120°C.

The cladding was done for all the eight blocks on both the surfaces. Precautions were taken to reduce the dilution to the minimum. However the original crack height got altered due to dilution. The final dimensions of the crack height was confirmed by radiography and recorded in Table 1, 2 and 3.

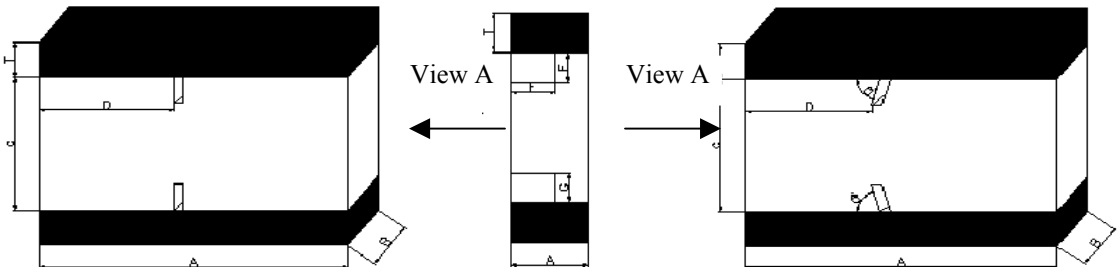

(a). Vertical cracks **(b). Inclined cracks**

Figure 2: Schematic diagram of the steel blocks showing the location and size of the subcladded vertical and inclined simulated cracks (slits)

Table 1: Dimensional detail of test blocks after embedment of the simulated vertical cracks (slits) by cladding

DIM / BL No.	Cladding material	A	B	C	D	E	F	G
BL.1	Inconel	248	39.8	36.08	124	20	4.56	-
BL.2	SS	247.5	39.8	46.78	128.75	25	8.44	1.88
BL.3	Ferritic	200	48.5	51.84	100	30	18.02	1.68
BL.4	Ferritic	250	39.10	68.08	125	25	13.72	3.51

Table 2: Dimensional details of test blocks after embedment of the simulated inclined cracks (slits) by cladding

DIM / BL No.	Cladding material	A	B	C	D	E	F	G*	θ^0
BL.5	SS	231.7	37	81.27	115.85	25	5.01	1.90	15
BL.6	Inconel	130.3	37.4	89.11	115.15	20	9.22	6.80	15
BL.7	Ferritic	225.3	41.3	141.50	112.65	25	14.30	11.93	10
BL.8	Ferritic	300.6	41	133.89	150.3	25	19.04	17.31	10

Note: All the dimensions are given in mm

* A - length, B - width, C - thickness, D - distance of the slit from one end of the block, E - length of the slit, F and G - height of the simulated cracks.

(a). Block as cladded **(b). Block after machining**

Figure 3: Embedment of simulated cracks (slits) by cladding

Table 3: Location details and actual dimensions of the simulated cracks (slits) after embedment by cladding

Cladding material	Block No.	Top surface cladding	Simulated Crack-1			Simulated Crack- 2			
			Depth of top tip	Depth of bottom tip	Crack height	Bottom surface cladding	Depth of top tip	Depth of bottom tip	Crack height
Vertical Cracks									
Inconel	01.	5.44	5.44	10	4.56	-	-	-	-
SS	02.	6.19	6.19	14.63	8.44	14.32	30.58	32.46	1.88
Ferritic	03.	7.24	7.24	25.26	18.02	9.58	40.58	42.26	1.68
Ferritic	04.	21.23	21.23	34.95	13.72	19.52	45.05	48.56	3.51
Inclined Cracks									
SS	05.	18.26	18.26	23.27	5.01	8.97	70.4	72.3	1.90
Inconel	06.	19.77	19.77	28.99	9.22	18.67	63.64	70.44	6.80
Ferritic	07.	10.87	10.87	25.17	14.30	19.39	110.18	122.11	11.93
Ferritic	08.	12.23	12.23	31.27	19.04	24.02	92.56	109.87	17.31

Observations: The experimental observations with respect to through thickness height and length of the simulated cracks are shown in Table 4 and the details of the cross-sectional size of the simulated cracks are shown in Table 5. Figures 4 and 5 gives the graphical representation of the actual Vs estimated height of the cracks. Table 6 shows the consolidated results of the experiments. Figures 6 and 7 gives the aspect ratio (actual Vs estimated) for vertical and inclined cracks respectively. Figures 8 shows the actual images of some of the vertical and inclined cracks.

Table 4: Estimation of through thickness height / length of simulated cracks (slits)

Actual crack height (mm)	Depth of top tip from scanning surface (mm)	TOF difference Δt (μ sec)	Measured height (mm)	Error in height (mm)	Actual crack length (mm)	Measured length (mm)	Error in length (mm)
Vertical Cracks							
1.68	40.58	1.25	2.76	1.08	20	19.84	-0.16
1.88	30.58	0.63	2.59	0.71			
3.51	45.05	0.88	3.52	0.01	25	24.35	-0.65
4.56	5.44	1.09	4.40	-0.16			
8.44	6.19	0.88	7.87	-0.57	30	29.76	-0.24
13.72	21.23	2.5	13.72	0			
18.02	7.24	2.77	18.20	0.18	25	23.45	-1.55
Inclined Cracks							
1.90	70.40	0.53	1.93	0.03	25	25.44	+0.44
5.01	18.26	0.5	5.20	0.19			
6.80	63.64	1.63	6.64	-0.16	20	21.73	+1.73
9.22	19.77	2.41	9.35	0.13			
11.93	10.87	3.66	11.50	-0.43	25	25.44	+0.44
14.30	110.18	1.40	14.08	-0.22			
17.31	92.56	3.78	16.68	-0.63	25	26.34	+1.34
19.04	12.23	3.34	19.04	0			

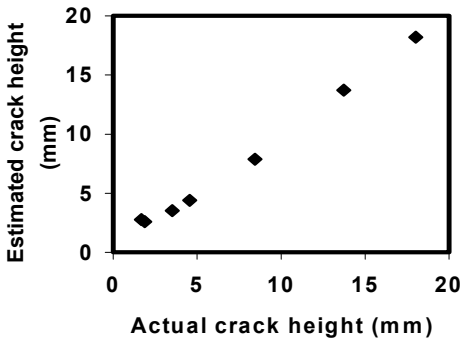

Figure 4: Estimation of through thickness height for vertical cracks

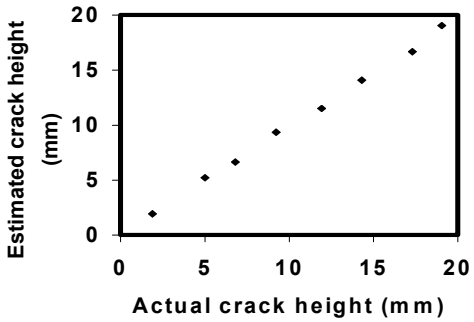

Figure 5: Estimation of through thickness height for inclined cracks

Table 5: Aspect Ratio

Vertical Cracks			Inclined Cracks		
Actual values	Estimated values	Error	Actual values	Estimated values	Error
0.08	0.14	0.06	0.08	0.08	0
0.09	0.13	0.04	0.20	0.20	0
0.14	0.15	0.01	0.34	0.30	0.04
0.18	0.18	0	0.46	0.43	0.03
0.28	0.26	-0.02	0.48	0.45	0.03
0.46	0.46	0	0.57	0.55	0.02
0.72	0.78	0.06	0.69	0.63	0.06
-	-	-	0.76	0.72	0.04

$$\text{Aspect Ratio} = \frac{\text{Height of the crack}}{\text{Length of the crack}}$$

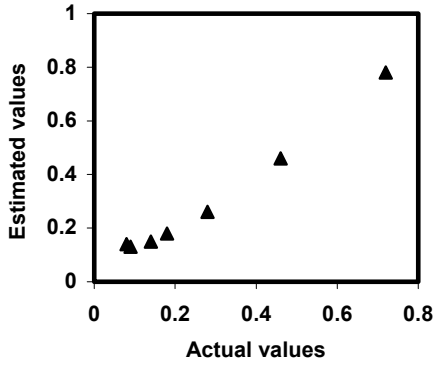

Figure 6: Aspect ratio for vertical cracks

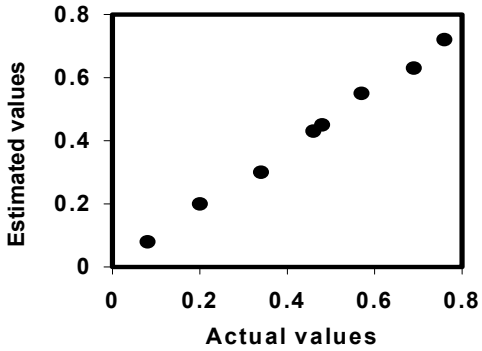

Figure 7: Aspect ratio for inclined cracks

Table 6: Consolidated Results

	Mean error		SD		Sample details	
	Vertical cracks	Inclined cracks	Vertical cracks	Inclined cracks	Vertical cracks	Inclined cracks
Through thickness height	0.18mm	-0.14mm	0.55	0.28	7	8
Length extremities	-0.65mm	0.99mm	0.64	0.65	4	4
Aspect ratio	0.02	0.03	0.03	0.02	7	8

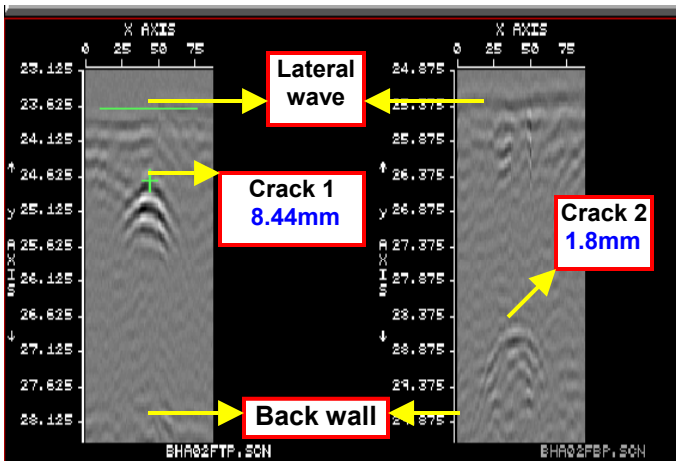

(a). Cracks under SS cladding

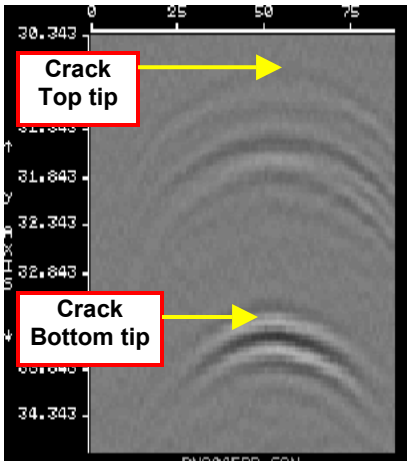

(b). Crack under Ferritic cladding

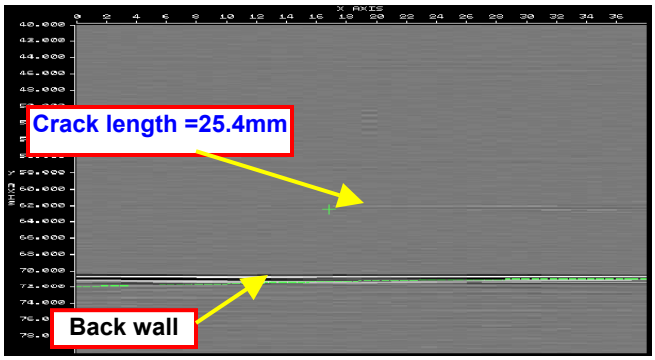

(c). Crack under Ferritic cladding

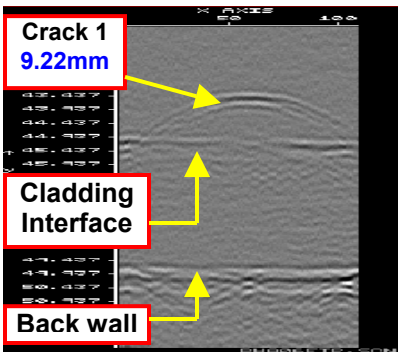

(d). Crack under Inconel cladding

Figure 8: TOFD images from vertical and inclined simulated cracks (slits)

Results and Discussion: The experimental results have shown excellent correlation between the actual and estimated through thickness height and length of the simulated cracks (slits). In case of the vertical slits the mean error is found to be ±0.18mm and the SD is 0.55 and in case of inclined slits the mean error is found to be ±0.14mm and the SD is 0.28. As can be seen from the results, the diffracted signal from the inclined slit (10° & 15°) are comparatively insensitive to angle and hence the diffraction technique is very good as a locator of the slits. This is because of the fact that the technique does not depend upon the amplitude of the signal. The proven level of accuracy attainable is found to be within ±0.2mm in terms of critical through wall extent and ±0.9mm in terms of horizontal dimension.

Since in TOFD, the estimate of the depth of a crack extremity below the inspection surface depends on the velocity of the various waves, it is necessary to correct for the effect of the variation of velocity in cladding. It is not practicable to measure the velocities for every ray path and the detailed cladding structure is both too complicated and too imperfectly known for exact calculations to be performed [(12)].

It has been observed that TOFD suffers from a near surface effect caused by its inherent lateral wave. Difficulty was experienced using TOFD to detect and size cracks starting from the interface between inconel /Stainless Steel cladding and the ferritic base i.e. (5mm/6mm below the scanning surface). This is due to lateral wave, which obscures the tip-diffracted signals from the defects close to the surface and also due to the inherent lack of time resolution near the surface. The investigations revealed that the width of the lateral wave for Stainless Steel and Inconel was 12mm and 18mm. However, these cracks could be well detected and sized by scanning through

the cladding from the opposite surface of the blocks. Even the small cracks of the order of 1.9mm could be detected as long as they are not influenced by the lateral wave. While testing from the clad surface, there is a shift, which was due to the inability of the 45° probes to resolve the signal from the top edge of the defect from cladding noise and internal echoes [14]. It was also observed that the untreated TOFD B-scan image does not show a reconstruction of the defect, but only possible locations of special points of defects. The problem has been solved by a Synthetic Aperture Focusing Algorithm (SAFT) [15].

Acknowledgement: Our sincere thanks to Council of Scientific & Industrial Research (CSIR), New Delhi, India for awarding the Senior Research Fellowship (SRF) to Ms. Sony Baby {Sanction No. 1(64) 010-2k2/1} and financially supporting her in the pursuance of her research study. The authors of the paper are thankful to the management of Bharat Heavy Electricals Limited, Tiruchirappalli and Indira Gandhi Centre for Atomic Research, Kalpakam, India for providing necessary equipments and facilities for carrying out this experimental work. Thanks are also due to all the concerned officers / technical staff particularly Shri. P.S. Subbaraman, Sr.Scientific officer, NDTL / BHEL, Tiruchirappalli who supported for this study.

References:

1. Sony Baby, Balasubramanian, T. and Pardikar, R.J., Estimation of the height of surface-breaking cracks using ultrasonic timing methods, Insight, Vol.44, No.11, Nov 2002, 679-683.
2. Sony Baby, Balasubramanian, T. and Pardikar, R.J., Time of flight diffraction technique for accurate sizing of surface breaking cracks, Insight, Vol., No., June 2003.
3. Diagiacomot, G, An ultrasonic method of measuring crack depth in structural weldments, Materials Evaluation, 28-9 (1970).
4. Katoh, I., Sakurai, Y and Matsumura, T, The measurement of flaw height by ultrasonic Testing, Hihakaikensa. Journal of NDI 26(5), 320-323 (1977).
5. Lidington, B. H and Silk, M.G, The potential of scattered or diffracted ultrasound in determination of crack depth, NND, 146 –151 (June 1975).
6. Date, K., Shimada, H. and Ikenaga, N, Crack height measurement – an Evaluation of the accuracy of ultrasonic timing methods, NDT International, 315-319 (Dec 1982).
7. Ogura, Y., A study on accuracy of ultrasonic determination of the height of defect, Journal of JSNDT 27(2), 118 – 119 (1978).
8. Silk, M.G., The propagation of ultrasound in austenitic weldments, Materials Evaluation, 39(5), 462-466.
9. Silk, M.G., Relationships between metallurgical texture and ultrasonic propagation, Met Science, 15(11-12), 559-565.
10. Silk, M. G., The propagation of polarized shear waves in steel, U.K.A.E.A. Report AERE-R 9423, Harwell Laboratory.
11. Silk, M. G., Ultrasonic techniques fro inspecting austenitic welds, Research techniques in Nondestructive Testing, Vol.4, Chapter, 11, 393-449. (Edited by R.S. Sharpe Academic Press, London, 1980.
12. Charlesworth, J. P, Temple J. A. G., Engineering Applications of Ultrasonic Time-of-Flight Diffraction, Research Studies Press Ltd., England.
13. Silk M G, The use of diffraction – based time-of-flight measurements to locate and size defects, British Journal of Non-destructive Testing, May 1984, 208-213.
14. Bowker, K.J., Coffey, J.M., Hanstock, D.J., Owen, R.C. and Wrigley, M., CEGB Inspection of Plates 1 and 2in UKAEA Defect Detection Trials, British Journal of NDT, September 1983, 249-255.
15. Udo Schelgermann, Can TOFD replace conventional ultrasonic testing on welding, NDTnet, May 23rd, 1997, Vol. 02, No 09.